Journal of Molecular and Cellular Cardiology xxx (2015) xxx–xxx

Contents lists available at ScienceDirect

Journal of Molecular and Cellular Cardiology

journal homepage: www.elsevier.com/locate/yjmcc

Original article

Increased LDL electronegativity in chronic kidney disease disrupts calcium homeostasis resulting in cardiac dysfunction☆

Kuan-Cheng Chang [a,b,1], An-Sheng Lee [c,d,1], Wei-Yu Chen [d], Yen-Nien Lin [a], Jing-Fang Hsu [d], Hua-Chen Chan [d,e], Chia-Ming Chang [d], Shih-Sheng Chang [a], Chia-Chi Pan [d], Tatsuya Sawamura [f], Chi-Tzong Chang [g], Ming-Jai Su [h,*], Chu-Huang Chen [d,i,j,k,**]

[a] Division of Cardiology, China Medical University (CMU) Hospital, Taichung, Taiwan
[b] Graduate Institute of Clinical Medical Science, CMU, Taichung, Taiwan
[c] Department of Medicine, Mackay Medical College, New Taipei, Taiwan
[d] L5 Research Center, CMU Hospital, CMU, Taichung, Taiwan
[e] Center for Lipid Biosciences, Kaohsiung Medical University (KMU) Hospital, KMU, Kaohsiung, Taiwan
[f] Department of Physiology, Shinshu University School of Medicine, Matsumoto, Nagano, Japan
[g] Division of Nephrology, CMU Hospital, Taichung, Taiwan
[h] Graduate Institute of Pharmacology, National Taiwan University, Taipei, Taiwan
[i] Vascular and Medicinal Research, Texas Heart Institute, Houston, TX, USA
[j] Department of Medicine, Baylor College of Medicine, Houston, TX, USA
[k] Center for Lipid and Glycomedicine Research, KMU Hospital, KMU, Kaohsiung, Taiwan

ARTICLE INFO

Article history:
Received 18 November 2014
Received in revised form 27 March 2015
Accepted 28 March 2015
Available online xxxx

Keywords:
Cardiorenal syndrome
Unilateral nephrectomy
Lipoproteins
SERCA2a

ABSTRACT

Chronic kidney disease (CKD), an independent risk factor for cardiovascular disease, is associated with abnormal lipoprotein metabolism. We examined whether electronegative low-density lipoprotein (LDL) is mechanistically linked to cardiac dysfunction in patients with early CKD. We compared echocardiographic parameters between patients with stage 2 CKD (n = 88) and normal controls (n = 89) and found that impaired relaxation was more common in CKD patients. Reduction in estimated glomerular filtration rate was an independent predictor of left ventricular relaxation dysfunction. We then examined cardiac function in a rat model of early CKD induced by unilateral nephrectomy (UNx) by analyzing pressure–volume loop data. The time constant of isovolumic pressure decay was longer and the maximal velocity of pressure fall was slower in UNx rats than in controls. When we investigated the mechanisms underlying relaxation dysfunction, we found that LDL from CKD patients and UNx rats was more electronegative than LDL from their respective controls and that LDL from UNx rats induced intracellular calcium overload in H9c2 cardiomyocytes *in vitro*. Furthermore, chronic administration of electronegative LDL, which signals through lectin-like oxidized LDL receptor-1 (LOX-1), induced relaxation dysfunction in wild-type but not LOX-1$^{-/-}$ mice. In *in vitro* and *in vivo* experiments, impaired cardiac relaxation was associated with increased calcium transient resulting from nitric oxide (NO)-dependent nitrosylation of SERCA2a due to increases in inducible NO synthase expression and endothelial NO synthase uncoupling. In conclusion, LDL becomes more electronegative in early CKD. This change disrupts SERCA2a-regulated calcium homeostasis, which may be the mechanism underlying cardiorenal syndrome.

Abbreviations: Apo, apolipoprotein; CKD, chronic kidney disease; EDPVR, end-diastolic pressure–volume relationship; ESPVR, end-systolic pressure–volume relationship; HDL, high-density lipoprotein; LDL, low-density lipoprotein; LOX-1, lectin-like oxidized LDL receptor-1; NO, nitric oxide; PV, pressure–volume; SERCA2a, sarco/endoplasmic reticulum Ca^{2+}-ATPase 2a; UNx, unilateral nephrectomy.

☆ The work described in this manuscript was presented in abstract form at the 2012 AHA Scientific Sessions.

* Correspondence to: M.-J. Su, Graduate Institute of Pharmacology, National Taiwan University, 1150R, No.1, Sec.1, Ren-Ai Rd., Taipei 100, Taiwan. Tel.: +886 2 23123456x88317; fax: +886 2 23971403.
** Correspondence to: C.-H. Chen, Vascular and Medicinal Research, Texas Heart Institute, 6770 Bertner Avenue, Houston, TX 77030, USA. Tel.: +1 832 355 9026; fax: +1 832-355-9333.
E-mail addresses: mingja@ntu.edu.tw (M.-J. Su), cchen@texasheart.org (C.-H. Chen).

[1] Kuan-Cheng Chang and An-Sheng Lee contributed equally to this work.

http://dx.doi.org/10.1016/j.yjmcc.2015.03.016
0022-2828/© 2015 Published by Elsevier Ltd.

1. Introduction

Primary disorders of the heart or kidney often result in secondary dysfunction of the other organ [1]. Chronic kidney disease (CKD) has been shown to be an independent risk factor for cardiovascular disease and is associated with increased cardiovascular morbidity and mortality [2]. Clinically, CKD can be classified into 5 stages according to the levels of glomerular filtration rate degradation [3]. Previous studies have shown that even patients with less severe CKD (stage 1 to 3) are at high cardiovascular risk [4] as the result of early cardiovascular remodeling [5]. A growing body of evidence suggests that impaired kidney function is associated with the release of humoral and/or cellular factors that may contribute to myocardial remodeling [6]; however, the underlying molecular mechanisms remain unclear.

Dyslipidemia is an important risk factor for the development and progression of both CKD and cardiovascular diseases [7]. In patients with CKD, dyslipidemia is characterized by high levels of triglyceride, low levels of high-density lipoprotein (HDL) cholesterol, and the accumulation of small dense low-density lipoprotein (LDL) particles. However, LDL cholesterol levels are usually normal in these patients. Nevertheless, it remains possible that the composition of LDL is altered in patients with CKD.

Human plasma LDL can be separated according to charge into 5 subfractions, called L1–L5. L5, the most electronegatively charged LDL subfraction, is highly atherogenic and has *in vitro* properties similar to those of oxidized LDL [8–10]. Importantly, L5 levels are elevated in individuals with risk factors for cardiovascular disease, such as hypercholesterolemia or diabetes, when compared with levels in healthy subjects, in whom L5 is undetectable or present in trace amounts [11,12]. Recently, we also found that the percentage of L5 in total LDL is higher in patients with ST-segment elevation myocardial infarction than in healthy individuals [13,14]. Thus, we hypothesized that altered LDL electronegativity may play a role in cardiovascular remodeling during the course of CKD. In this study, we compared echocardiographic parameters between patients with early CKD and individuals with normal kidney function to show that patients with early CKD exhibit relaxation dysfunction. We also characterized cardiac structural and functional changes in a rat model of early-stage CKD induced by unilateral nephrectomy (UNx). To identify a mechanistic link between early CKD and cardiac remodeling, we examined the properties of LDL isolated from patients with CKD and from UNx rats and assessed the cardiac structural and functional changes in an L5-injected mouse model to establish the importance of electronegative LDL in promoting cardiac dysfunction.

2. Materials and methods

2.1. Study subjects

All human research performed in this study conformed to the ethical guidelines of the 1975 Declaration of Helsinki as reflected in *a priori* approval by the China Medical University Hospital-Taiwan Institutional Review Board (CMUH103-REC1-070 [AR-1]). We retrospectively enrolled 88 consecutive ambulatory patients with stage 2 CKD [3] who were referred for echocardiography examination. For a control group, we randomly selected 89 age- and sex-matched individuals with normal kidney function. Clinical and echocardiographic data were obtained from the electronic medical records database and were analyzed anonymously to maintain confidentiality. For the retrospective data analysis, the institutional review board waived the requirement to obtain informed consent. Estimated glomerular filtration rate was determined by using the Modification of Diet in Renal Disease equation [3].

2.2. Animal models

All animal experiments were approved by the Institutional Animal Care and Use Committee of the China Medical University (101-159-N) and were performed in accordance with the ARRIVE guidelines and the guidelines set by the National Institutes of Health for the care and use of laboratory animals. The rats and C57B6/J mice used in this study were purchased from BioLASCO Taiwan Co., Ltd. (Taipei, Taiwan). To characterize the cardiac structural and functional changes in an animal model of early CKD, we used a rat model of early CKD induced by UNx. Forty adult male 8-week-old Sprague–Dawley rats were assigned to 1 of 2 groups: the UNx group (n = 20) or the sham group (ie, sham-operated, n = 20). Rats in the UNx group underwent removal of the left kidney following ligation of the left renal artery. For these operations, the animals were anesthetized with 2% isoflurane (Abbott, Abbott Park, IL) and supported by a rodent ventilator (New England Medical Instruments, Inc., Medway, MA). To determine the effect of exogenous L5 on cardiac function, 8-week-old C57B6/J mice (wild-type mice) were injected with 1 mg/kg of L1 or L5 (n = 5 per group) through the tail vein every day for 4 weeks. LOX-1$^{-/-}$ mice (n = 5), a gift from Dr. Tatsuya Sawamura (National Cerebral and Cardiovascular Center, Japan), were also injected with L5 daily for 4 weeks to determine the role of LOX-1. We also compared the LDL electronegativity on agarose gel electrophoresis and the diastolic function of LOX-1$^{-/-}$ mice that underwent UNx or a sham operation (n = 3 per group). At the end of the experiments, the animals were anesthetized with 5% isoflurane and euthanized *via* cervical dislocation.

2.3. Echocardiographic examination

For the CKD patients and control individuals, an echocardiographic examination was performed according to standard protocols [15]. For the UNx and sham rats, transthoracic echocardiography was performed immediately before and 8 weeks after the operation in both short- and long-axis views by using GE Velocity Vector Imaging (GE Medical Systems, Milwaukee, WI) with probe 10S.

2.4. In vivo pressure–volume loop analysis

Animals were anesthetized with 4% isoflurane and were supported by a ventilator with a maintenance dose of 2% isoflurane after tracheostomy. A P–V catheter (2.0 F for rats and 1.4 F for mice) was inserted into the left ventricle through the right carotid artery. Signals of pressure and volume were continually recorded by using a P–V conductance system (MPVS Ultra, emka TECHNOLOGIES, Paris, France) coupled to a digital converter (ML-870, ADInstruments, Colorado Springs, CO). Hemodynamic parameters were measured under different preloads, which were elicited by transiently compressing the abdominal inferior vena cava.

2.5. LDL isolation and determination of LDL electronegativity

Human, rat, and mouse plasma LDL samples were isolated by using sequential potassium bromide density-gradient ultracentrifugation. LDL samples were separated in 0.7% agarose by using electrophoresis, and the delipidated LDL samples were subjected to sodium dodecyl sulfate polyacrylamide gel electrophoresis. LDL subfractions isolated from humans and separated according to electrical charge were further separated and collected by using fast protein liquid chromatography (GE Health Care, Buckinghamshire, UK) with UnoQ12 anion-exchange columns (BioRad, Inc., Hercules, CA), as described previously [8–10].

2.6. Cell study

H9c2 rat cardiomyocytes were purchased from Bioresource Collection and Research Center (Food Industry Research and Development Institute,

Please cite this article as: Chang K-C, et al, Increased LDL electronegativity in chronic kidney disease disrupts calcium homeostasis resulting in cardiac dysfunction, J Mol Cell Cardiol (2015), http://dx.doi.org/10.1016/j.yjmcc.2015.03.016

Taiwan) and maintained in Dulbecco's modified Eagle's medium (Gibco/Invitrogen) supplemented with 10% fetal bovine serum and 1% penicillin/streptomycin/neomycin mixture (Gibco/Invitrogen). Subconfluent H9c2 cardiomyocytes were exposed to 100 μg/mL LDL from sham or UNx rats for 24 h.

2.7. Immunoblotting and immunoprecipitation analysis

Protein extracts from either H9c2 cells or rodent ventricles were used for immunoblotting and immunoprecipitation analysis. H9c2 cells were lysed in RIPA buffer (Pierce Biotechnology, Inc., Rockford, IL) with protease inhibitor cocktail, and the left ventricle of each animal was homogenized by using a Mini-Beadbeater-1 (Biospec Products, Inc.) in T-PER Tissue Protein Extraction Reagent. Protein concentrations were measured by using a BCA assay (Pierce). For immunoblotting, we used polyclonal antibodies against iNOS (Santa Cruz Biotechnology), LOX-1 (Biorbyt), SERCA2a (Cell Signaling Technology), nitrotyrosine (Cell Signaling Technology), and β-actin (Sigma Aldrich). For the immunoprecipitation experiments, Qbeads-IgG (MagQu Co.) were bound to anti-SERCA2a antibody and then incubated with ventricular protein extract. The immunoprecipitates were collected by using magnetic beads.

2.8. Isolation of ventricular myocytes

Left ventricular myocytes were enzymatically isolated by using the Langendorff perfusion method. Animal hearts were retrogradely perfused with Krebs buffer (120 mmol/L NaCl, 12 mmol/L glucose, 25 mmol/L $NaHCO_3$, 1.2 mmol/L KH_2PO_4, 1.2 mmol/L $MgSO_4$, and 5.4 mmol/L KCl; pH = 7.4 [adjusted by using HEPES]). After 5 min of equilibration, 0.4 mg/mL collagenase (type II, Worthington) was added for 20 min. Hearts were then cut into small pieces and digested with 0.4 mg/mL collagenase and 0.02 mg/mL trypsin (Gibco) in Krebs buffer for 20 min. After filtration, myocytes were washed with Krebs buffer twice and stored in Dulbecco's modified Eagle medium (Gibco/Invitrogen).

2.9. Calcium transient recording

Myocytes were loaded with 0.5 μmol/L fura-2-acetoxymethyl ester (Molecular Probes). Measurements of myocyte shortening and calcium transient were conducted simultaneously by using the Myocytes Calcium and Contractility Recording System (IonOptix).

2.10. Uncoupled eNOS measurement by low-temperature sodium dodecyl sulfate polyacrylamide gel electrophoresis

The ventricular protein extracts were mixed with 3× sodium dodecyl sulfate (SDS) sample buffer (190 mmol/L Tris–HCl [pH 6.8], 6% wt/vol SDS, 30% glycerol, 15% vol/vol 2-mercaptoethanol) at 0 °C and then loaded on 7.5% polyacrylamide gels. Electrophoresis was performed in an ice bath, and the eNOS dimer and monomer proteins were detected by Western blot analysis with eNOS antibody (Santa Cruz Biotechnology).

2.11. Assessment of cardiac fibrosis via pathologic analysis and measurement of early fibrosis markers

Sham and UNx rat hearts were fixed in formalin, dehydrated, and embedded in paraffin. Both Masson's trichrome and picrosirius red staining were used to accurately estimate the degree of fibrosis. All samples were analyzed by an experienced pathologist who was blinded to the different groups of animals. Semi-quantitative RT-PCR was performed to measure mRNA expression levels of early fibrosis markers. For this analysis, the following sense and antisense primers were used: 5′-GACCTCATGTTCATCTTTAGA-3′ (sense) and 5′-CACCACAATAAGGA ATTCGTT-3′ (antisense) for MMP-1, 5′-TGGCTTCTGGCATCCTGTTGTTG-3′ (sense) and 5′-TGGACACTGTGCAGGCTTCACTT-3′ (antisense) for TIMP-1, and 5′-TCTTCACCACCATGGAGAA-3′ (sense) and 5′-ACTGTGGT CATGAGCCCTT-3′ (antisense) for GAPDH.

2.12. Measurement of renin, angiotensin II, and aldosterone levels

Because chronic kidney disease is associated with the expression of the renin–angiotensin system, we determined serum levels of renin, angiotensin II, and aldosterone protein in the serum of 20 individuals with stage 2 CKD (eGFR, 60–89 mL/min/1.73 m^2) and 33 age- and sex-matched controls (eGFR ≥ 90 mL/min/1.73 m^2). We also compared serum angiotensin II and aldosterone levels between sham-operated and UNx rats and between L1- and L5-injected wild-type mice and L5-injected LOX-$1^{-/-}$ mice (n = 5 per group). Serum protein levels were analyzed by using human renin (Quantikine; R&D Systems Inc., Minneapolis, Minnesota, USA), angiotensin II (Cloud-Clone Corp., Houston, Texas, USA), and aldosterone enzyme-linked immunosorbent assay (ELISA) kits (Abnova, Walnut, California, USA). All protein levels were measured according to the manufacturer's instructions.

2.13. Data analysis and statistics

For the human studies, continuous data are expressed as the mean ± standard deviation. The significance of the difference between 2 groups was determined by using a Student *t* test. Odds ratios and 95% confidence intervals were calculated by performing univariate and multivariate logistic regression analyses. For categorical variables, the difference between proportions was assessed by using a chi-squared or Fisher's exact test. For the animal and cell experiments, data are expressed as the mean ± standard error of the mean (SEM), and the difference between 2 groups was determined by using the Mann–Whitney U test. *P* values <0.05 were considered statistically significant.

3. Results

3.1. Patients with early CKD showed evidence of relaxation dysfunction

Table 1 shows demographic, clinical, and echocardiographic data for 88 patients with early CKD and 89 age- and sex-matched controls with normal kidney function. The estimated glomerular filtration rate (eGFR) was significantly lower in patients with early CKD than in controls ($P < 0.001$). In addition, the mean mitral E and E/A values were significantly lower in patients with early CKD than in controls (both $P < 0.01$), and the mitral E deceleration time was significantly longer in patients with early CKD ($P = 0.02$). Furthermore, the presence of diastolic dysfunction of any degree was more common in patients with early CKD than in controls ($P < 0.01$).

Logistic regression analysis revealed that reduced eGFR was an independent predictor of left ventricular diastolic dysfunction (adjusted odds ratio, 0.94; 95% confidence interval, 0.91–0.98; $P < 0.01$) after accounting for other covariates including age, history of hypertension, heart rate, and aspartate aminotransferase level (Table S1).

3.2. UNx rats exhibited relaxation dysfunction

Unilateral nephrectomy was performed in 20 adult Sprague–Dawley rats to create a rat model of early-stage CKD, and 20 rats that underwent a sham operation were used as controls. Eight weeks after the operation, blood urea nitrogen and creatinine levels were moderately increased in UNx rats when compared with the levels in sham rats (Table S2).

Echocardiographic measurements revealed a significantly longer deceleration time of the mitral E wave in UNx rats than in sham rats ($P = 0.004$; Fig. 1A and Table S3). In pressure–volume (P–V) loop experiments, the systolic and diastolic functions of the rat hearts were evaluated *in vivo* at different preloads (Fig. 1B). The slopes of both the

Please cite this article as: Chang K-C, et al, Increased LDL electronegativity in chronic kidney disease disrupts calcium homeostasis resulting in cardiac dysfunction, J Mol Cell Cardiol (2015), http://dx.doi.org/10.1016/j.yjmcc.2015.03.016

Table 1
Demographic, clinical, and echocardiographic characteristics of patients with early CKD and of normal controls.

Variables	Control (n = 89)	Early CKD (n = 88)	*P* value
Age (years)	43.02 ± 8.23	44.02 ± 6.76	0.38
Sex			0.76
Male	67 (75.3%)	68 (77.3%)	
Female	22 (24.7%)	20 (22.7%)	
Smoking status			0.41
No	83 (93.3%)	79 (89.8%)	
Yes	6 (6.7%)	9 (10.2%)	
Diabetes			**<0.01**
No	81 (91.0%)	88 (100.0%)	
Yes	8 (9.0%)	0 (0.0%)	
Hypertension			0.46
No	79 (88.8%)	81 (92.0%)	
Yes	10 (11.2%)	7 (8.0%)	
Body mass index (kg/m^2)	24.45 ± 3.50	24.24 ± 3.02	0.67
Systolic blood pressure (mm Hg)	122.69 ± 13.20	123.24 ± 15.19	0.80
Diastolic blood pressure (mm Hg)	77.37 ± 10.66	78.60 ± 11.16	0.45
Heart rate (beats/min)	65.90 ± 10.28	67.28 ± 11.55	0.41
Creatinine (mg/dL)	0.76 ± 0.14	0.98 ± 0.15	**<0.001**
eGFR (mL/min/1.73 m^2)	105.79 ± 13.78	79.60 ± 7.08	**<0.001**
Cholesterol (mg/dL)	210.65 ± 37.53	202.40 ± 30.04	1.00
Triglyceride (mg/dL)	150.24 ± 109.35	122.01 ± 64.15	0.40
Aspartate aminotransferase (IU/L)	24.91 ± 8.87	29.40 ± 18.04	0.95
Hemoglobin (g/dL)	14.95 ± 3.62	14.76 ± 1.59	0.95
LVEDD (mm)	48.55 ± 4.56	48.04 ± 5.05	0.42
LVESD (mm)	29.82 ± 3.85	29.56 ± 4.07	0.38
LVEF (%)	62.06 ± 5.61	61.98 ± 5.81	0.57
LVM (g)	116.79 ± 35.96	115.70 ± 32.16	0.57
LA (mm)	34.42 ± 5.10	34.06 ± 5.92	0.93
Mitral E deceleration time (ms)	207.41 ± 44.11	224.42 ± 51.68	**0.02**
Mitral E (m/s)	0.75 ± 0.15	0.68 ± 0.16	**<0.01**
Mitral A (m/s)	0.60 ± 0.15	0.61 ± 0.14	0.61
Mitral E/A	1.34 ± 0.45	1.17 ± 0.38	**<0.01**
Systolic velocity (S′) (cm/s)	7.88 ± 1.23	7.67 ± 1.15	0.24
Early diastolic velocity (E′) (cm/s)	9.59 ± 2.38	8.90 ± 2.09	**0.04**
Late diastolic velocity (A′) (cm/s)	8.55 ± 1.57	8.74 ± 1.67	0.44
Mitral E/E′	8.05 ± 1.92	7.92 ± 2.11	0.67
E′/A′	1.19 ± 0.47	1.07 ± 0.38	0.06
Diastolic dysfunction			**<0.01**
Normal	75 (84.3%)	57 (64.8%)	
E/A reverse	13 (15.7%)	31 (35.2%)	
Pseudonormalization	0	0	
Restrictive	0	0	

All values are expressed as mean ± standard deviation or n (%). eGFR, estimated glomerular filtration rate; LVEDD, left ventricular end-diastolic dimension; LVESD, left ventricular end-systolic dimension; LVEF, left ventricular ejection fraction; LVM, left ventricular mass; LA, left atrium; S′, the peak velocity of septal mitral annulus at systole; E′, the peak velocity of septal mitral annulus at early diastole; A′, the peak velocity of septal mitral annulus at late diastole.

end-systolic P–V relationship (ESPVR) and the end-diastolic P–V relationship (EDPVR) were not significantly different between UNx and sham rats (Fig. 1C). End-systolic pressure (Pes) and volume (Ves), end-diastolic pressure (Ped) and volume (Ved), maximal velocity of pressure rise (+dP/dt), maximal velocity of volume rise (+dV/dt) and fall (−dV/dt), and arterial elastance (Ea) were similar between UNx and sham rats (Figs. 1D–F). However, the maximal velocity of pressure fall (−dP/dt) was slower ($P = 0.045$; Fig. 1E) and the time constant of isovolumic pressure decay (tau) was longer ($P = 0.045$; Fig. 1F) in UNx rats than in sham rats, suggesting impaired active relaxation during early diastole.

3.3. Electronegative LDL isolated from UNx rats induced lectin-like oxidized LDL receptor-1 (LOX-1) and inducible nitric oxide synthase (iNOS) expression, SERCA2a nitrosylation, and calcium overload in H9c2 rat cardiomyocytes

Although the LDL levels in UNx and sham rats were comparable (Table S2), the LDL from UNx rats was more electronegative (Fig. 2A) and showed alterations in apolipoprotein (Apo) content (Fig. 2B). LDL from UNx rats was richer in ApoE, ApoAI, ApoCIII, and ApoCI proteins than LDL from sham rats. When H9c2 cardiomyocytes were incubated with 100 μg/mL LDL from UNx or sham rats, LDL from UNx rats induced higher expression of LOX-1 (a receptor for the most electronegative subfraction of LDL, L5) and iNOS than did LDL from sham rats ($P = 0.007$ and $P = 0.029$, respectively; Fig. 2C). This signaling may account for the increase of SERCA2a nitrosylation in cardiomyocytes treated with LDL from UNx rats ($P = 0.024$, Fig. 2D). LDL from UNx rats also induced a greater increase in intracellular calcium than did LDL from sham rats ($P = 0.047$) by prolonging the decay tau of calcium transient ($P = 0.045$) (Fig. 2E). Altogether, our results suggest that changes in the composition and electronegativity of LDL play an important role in the development of cardiac relaxation dysfunction caused by intracellular calcium overload.

3.4. LDL isolated from patients with early CKD was more electronegative than that from normal controls

To determine the clinical relevance of our findings, we compared the electronegativity and subfraction composition of LDL between healthy subjects and patients with early CKD. The results of agarose gel electrophoresis showed that the LDL from CKD patients was more electronegative than that from healthy controls (Fig. 3A). Furthermore, the percentage of L5 in total LDL was significantly higher in the serum from patients with early CKD than in that from controls (0.82 ± 0.12% *vs.* 0.41 ± 0.05%, $P = 0.001$; Fig. 3B).

3.5. Electronegative LDL induced relaxation dysfunction in mice via LOX-1

To further establish the role of electronegative LDL in CKD-induced cardiac relaxation dysfunction, we intravenously injected wild-type mice with low doses of L1 or L5 (n = 5 per group) for 4 weeks and then examined their cardiac function by performing P–V loop analysis. Additionally, LOX-1 knockout (LOX-1$^{-/-}$) mice (n = 5) were injected with L5 to determine the role of LOX-1. Fig. 4A shows representative results of the P–V loop analyses with different preloads in the L1- and L5-injected wild-type mice and L5-injected LOX-1$^{-/-}$ mice. The slopes of the ESPVR and EDPVR curves were not significantly different among the 3 groups of mice (Fig. 4B). Likewise, Pes, Ves, Ped, Ved, +dP/dt, +dV/dt, −dV/dt, and Ea were all similar among the 3 groups of mice (Figs 4C–E). However, the −dP/dt was smaller ($P = 0.049$, Fig. 4D) and the tau was greater ($P = 0.049$, Fig. 4E) in L5-treated wild-type mice than in L1-treated wild-type mice, but the effect of L5 was attenuated in LOX-1$^{-/-}$ mice. This suggests that the cardiac relaxation dysfunction seen in wild-type mice injected with L5 is similar to that seen in UNx rats and that it occurs *via* a LOX-1-dependent signaling pathway. Furthermore, we also compared the LDL electronegativity and diastolic function of LOX-1$^{-/-}$ mice that underwent UNx or a sham operation. We found that the LDL from LOX-1$^{-/-}$ mice that underwent UNx was more electronegative than that from the sham-operated LOX-1$^{-/-}$ mice. However, indicators of diastolic function, such as the slope of EDPVR, decay tau, and other parameters assessed in the P–V loop analysis were similar for both groups of mice (Fig S2). These findings support the notion that electronegative LDL-mediated diastolic dysfunction induced by UNx occurs *via* a LOX-1-dependent pathway.

3.6. Calcium transient was increased in cardiomyocytes from UNx rats and L5-injected wild-type mice due to prolonged decay tau

We examined whether calcium transient is altered in cardiomyocytes from UNx rats and L5-injected wild-type mice. We found that intracellular calcium levels were greater and the decay time of calcium transient (tau) was longer in cardiomyocytes from UNx rats than in those from sham rats ($P = 0.04$ and $P = 0.01$, respectively; Fig. 5A). In addition,

Please cite this article as: Chang K-C, et al, Increased LDL electronegativity in chronic kidney disease disrupts calcium homeostasis resulting in cardiac dysfunction, J Mol Cell Cardiol (2015), http://dx.doi.org/10.1016/j.yjmcc.2015.03.016

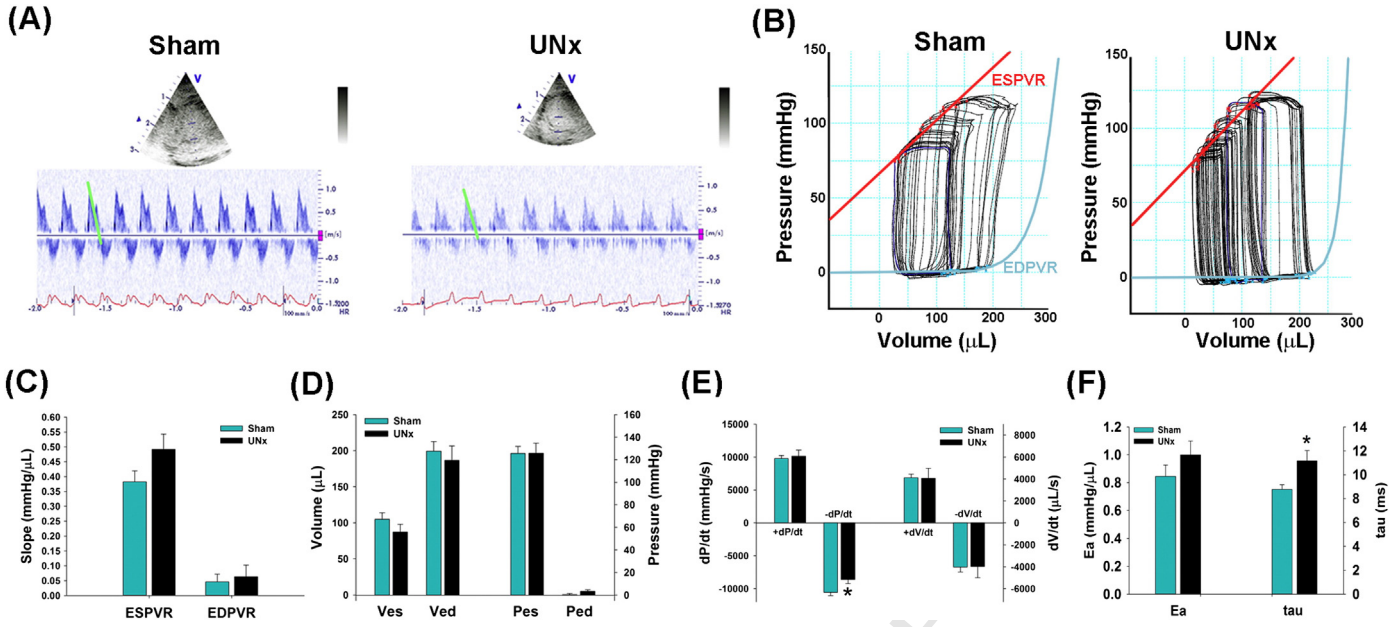

Fig. 1. Relaxation dysfunction in UNx rats. A, Representative echocardiograms showing a longer mitral deceleration time in an UNx rat than in a sham rat. B, Representative P–V loops at different preloads showing no significant differences in either the end-systolic P–V relationship (ESPVR) or the diastolic P–V relationship (EDPVR) between UNx and sham rats. C, Comparison of the mean slopes of the ESPVR and the EDPVR in UNx and sham rats. D, Comparison of the mean end-systolic volume (Ves), end-diastolic volume (Ved), end-systolic pressure (Pes), and end-diastolic pressure (Ped) in UNx and sham rats. E, Comparison of the maximal velocity of pressure rise (+dP/dt) and fall (−dP/dt) and the maximal volume rise (+dV/dt) and fall (−dV/dt) in UNx and sham rats. F, Comparison of the mean arterial elastance (Ea) and isovolumic relaxation constant (tau) in UNx and sham rats. For the quantitative analyses, n = 10 per group.*$P < 0.05$ *vs.* sham rats.

compared to L1 injections, L5 injections significantly increased intracellular calcium transient in cardiomyocytes from wild-type mice ($P = 0.034$) by prolonging the decay tau ($P = 0.001$), but these L5-induced effects were not seen in cardiomyocytes from LOX-1$^{-/-}$ mice (Fig. 5B).

3.7. LOX-1 expression and nitric oxide synthase-dependent nitrosylation of SERCA2a were upregulated in UNx rats and L5-injected wild-type mice

To determine the mechanism underlying the increased calcium transient in the UNx rats and L5-injected wild-type mice, we examined the expression levels of LOX-1 and iNOS and the degree of endothelial nitric oxide synthase (eNOS) uncoupling and SERCA2a nitrosylation in ventricular tissue. We found that the levels of LOX-1, iNOS, and uncoupled eNOS were higher in UNx rats than in sham rats ($P = 0.014$, $P = 0.049$, and $P = 0.002$, respectively) and higher in L5-injected wild-type mice than in L1-injected mice ($P = 0.029$ for all 3 comparisons) (Figs. 6A–D). Furthermore, the amount of nitrotyrosine co-immunoprecipitated with SERCA2a was higher in UNx rats and L5-injected wild-type mice than in their respective controls ($P = 0.048$ and $P = 0.001$, respectively; Figs 6E and F). Additionally, the upregulation of iNOS and LOX-1 expression, eNOS uncoupling, and SERCA2a nitrosylation seen in L5-injected wild-type mice was attenuated in L5-injected LOX-1$^{-/-}$ mice.

3.8. UNx rat hearts did not exhibit fibrosis

Hearts from the UNx and sham rats showed no significant myocardial fibrosis when stained with either Masson's trichrome or picrosirius red, and they exhibited comparable expression levels of MMP-1 and TIMP-1, which are early markers of fibrosis (Fig S1). These results indicate that the diastolic dysfunction observed in UNx rat hearts occurred independently of fibrosis.

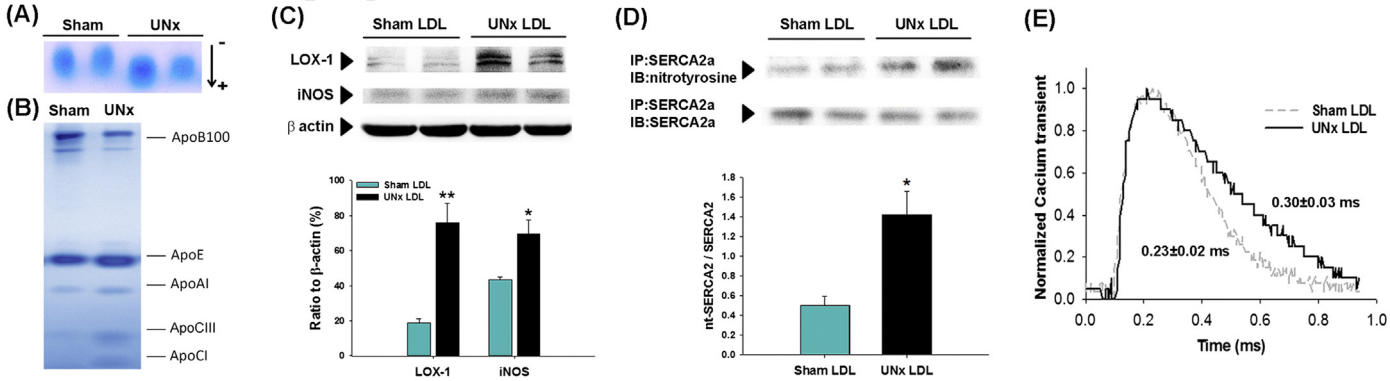

Fig. 2. Electronegativity of LDL isolated from UNx rats and its effects on H9c2 cardiomyocytes. Representative results of (A) agarose gel electrophoresis and (B) sodium dodecyl sulfate polyacrylamide gel electrophoresis of LDL isolated from UNx and sham rats. C, Western blot showing LOX-1 and iNOS expression in H9c2 cardiomyocytes treated with 100 μg/mL LDL from UNx or sham rats. D, Western blot showing the co-immunoprecipitation of nitrotyrosine with SERCA2a (top panel) and the quantitative analysis of the ratio of nt-SERCA2a to SERCA2a (bottom panel). E, Superimposed recordings of calcium transient in H9c2 cardiomyocytes treated with LDL from UNx or sham rats. The decay tau of the calcium transient is shown in the figure as mean ± SEM. For the quantitative analyses, n = 6 per group. *$P < 0.05$, **$P < 0.02$ *vs.* sham rats.

Please cite this article as: Chang K-C, et al, Increased LDL electronegativity in chronic kidney disease disrupts calcium homeostasis resulting in cardiac dysfunction, J Mol Cell Cardiol (2015), http://dx.doi.org/10.1016/j.yjmcc.2015.03.016

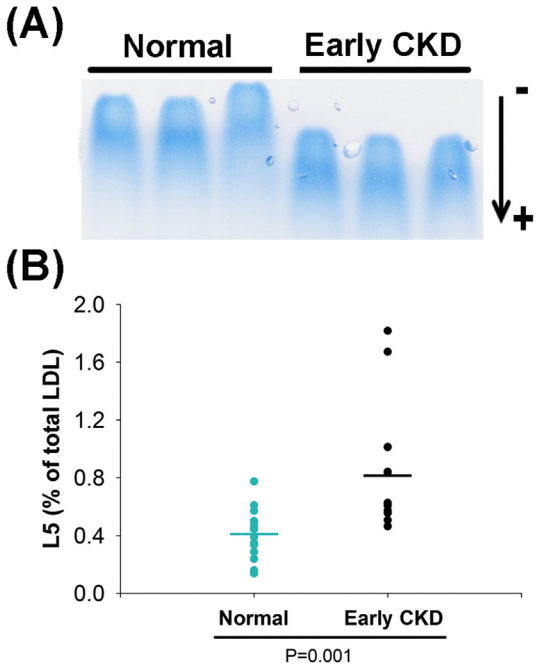

Fig. 3. Electronegativity of LDL isolated from patients with early CKD and healthy controls. A, Representative results of agarose gel electrophoresis of LDL from patients with early CKD and from normal controls. B, Percentage of L5 in total LDL for patients with early CKD and for normal controls. Lines indicate the mean value (n = 13 per group).

3.9. No change was seen in the renin–angiotensin system in early-stage CKD

The renin–angiotensin system is thought to play a key role in mediating myocardial changes associated with chronic kidney disease. Therefore, we examined plasma levels of renin, angiotensin II, and aldosterone in 20 individuals with stage 2 CKD (eGFR, 60–89 mL/min/1.73 m^2) and 33 age- and sex-matched controls (eGFR ≥90 mL/min/1.73 m^2). We found that the levels of all 3 component hormones of the renin–angiotensin system were comparable between the individuals with CKD and those without CKD (Fig S3). We also compared the angiotensin II and aldosterone levels between sham-operated and UNx rats and between L1- and L5-injected wild-type mice and L5-injected LOX-1$^{-/-}$ mice. Similar to the results for humans, no significant differences in the levels of these hormones were found between the animal models of early-stage CKD and their respective controls (Fig S3).

4. Discussion

In the current study, we show that relaxation dysfunction occurs as an early sign of cardiac remodeling in patients and rats with early CKD. The relaxation dysfunction that we observed may be mechanistically linked to abnormalities in calcium handling secondary to the peroxynitrite-dependent nitrosylation of SERCA2a. Importantly, we demonstrate for the first time, to our knowledge, that highly electronegative LDL may play a pivotal role in the development of cardiac relaxation dysfunction in patients with CKD. A schematic illustration depicting the potential mechanisms underlying CKD-induced cardiac relaxation dysfunction is shown in Fig. 7.

Intracellular calcium has an important role in regulating cardiac contraction and relaxation, and impaired calcium homeostasis has been shown to contribute to relaxation dysfunction [16]. In cardiomyocytes, an increase in nitrotyrosine/SERCA2a content or exposure to peroxynitrite causes inactivation of SERCA2a, which in turn leads to impaired calcium re-uptake into the sarcolemma reticulum [17]. A number of studies have shown that increases in iNOS and uncoupled eNOS result in the formation of superoxide, which is harmful to the cardiovascular system, instead of nitric oxide [18]. In myocytes from UNx rats, we found that iNOS and uncoupled

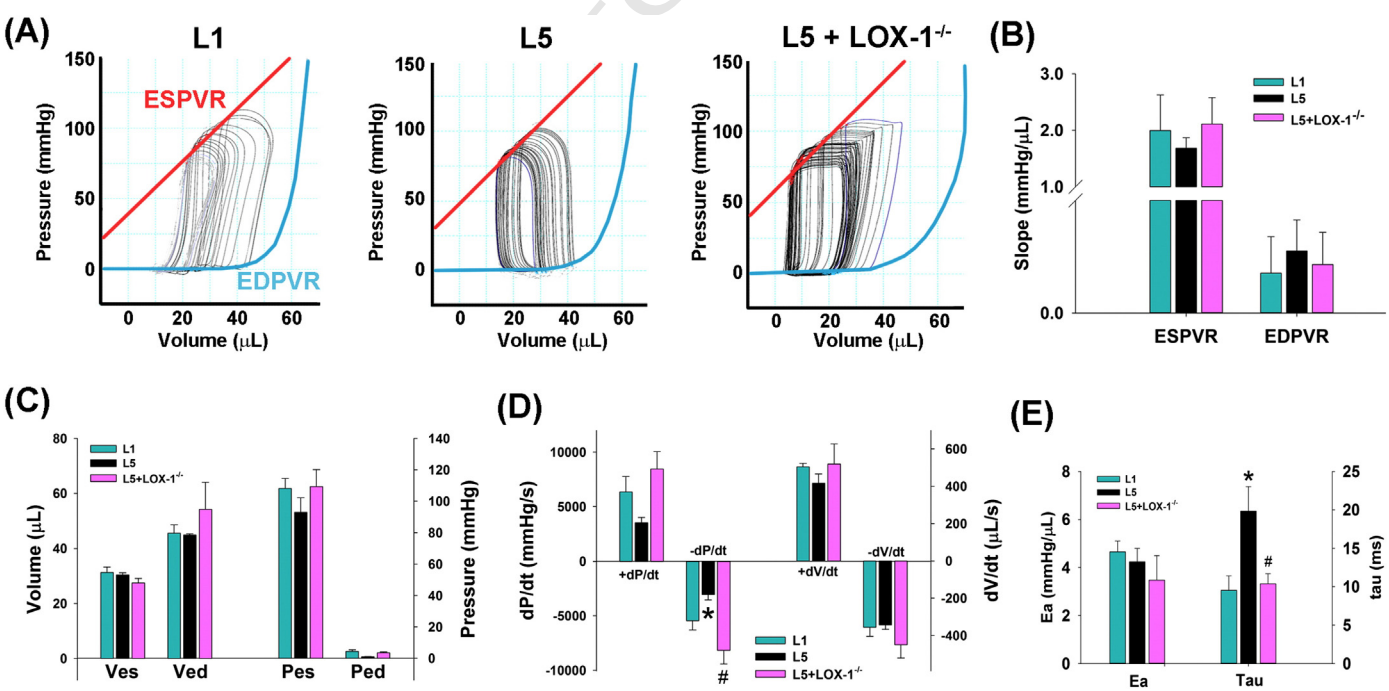

Fig. 4. Relaxation dysfunction in L5-injected wild-type mice. A, Representative P–V loops at different preloads showing no significant differences in either ESPVR or EDPVR among C57B6/J mice injected with L1 or L5 (1 mg/kg/day for 4 weeks) and LOX-1$^{-/-}$ mice injected with L5. B, The mean slopes of the ESPVR and the EDPVR are shown for the 3 mouse models. C, Comparison of the mean end-systolic volume (Ves), end-diastolic volume (Ved), end-systolic pressure (Pes), and end-diastolic pressure (Ped) in the 3 mouse models. D, Comparison of the maximal velocity of pressure rise (+dP/dt) and fall (−dP/dt) and the maximal volume rise (+dV/dt) and fall (−dV/dt) in the 3 mouse models. E, Comparison of the mean arterial elastance (Ea) and the time constant of isovolumic pressure decay (tau) in the 3 mouse models. For the quantitative analyses, n = 4 per group. *$P < 0.05$ *vs.* L1-injected wild-type mice; #$P < 0.05$ *vs.* L5-injected wild-type mice.

Please cite this article as: Chang K-C, et al, Increased LDL electronegativity in chronic kidney disease disrupts calcium homeostasis resulting in cardiac dysfunction, J Mol Cell Cardiol (2015), http://dx.doi.org/10.1016/j.yjmcc.2015.03.016

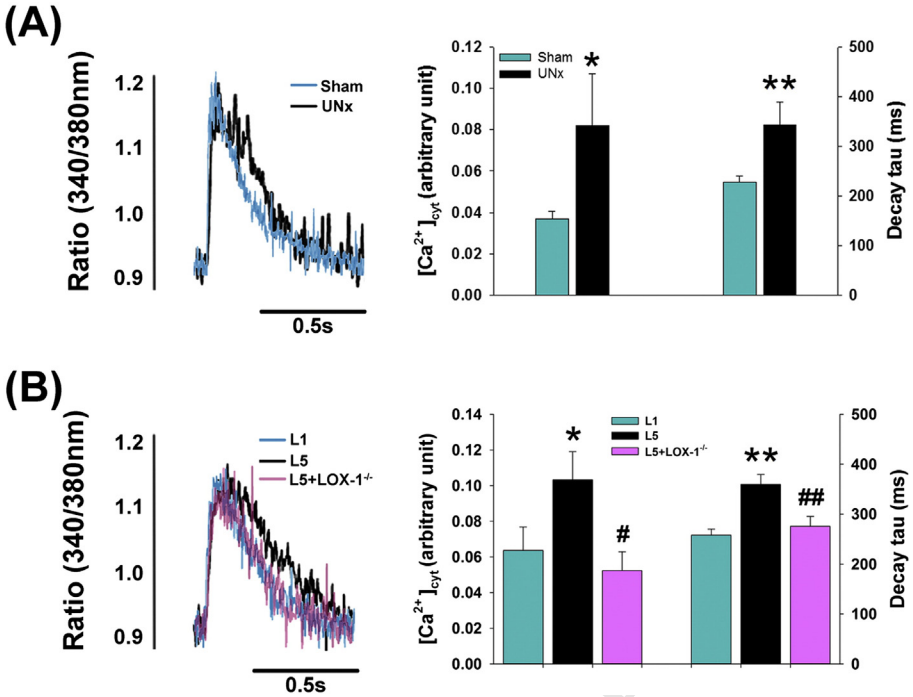

Fig. 5. Increased intracellular calcium transient in cardiomyocytes from UNx rats and L5-injected wild-type mice. Superimposed recordings of calcium transient in cardiomyocytes isolated from (A) sham and UNx rats and from (B) wild-type mice injected with L1 or L5 and LOX-1$^{-/-}$ mice injected with L5. The panels on the right show the quantification of intracellular calcium and the decay tau of calcium transient (n = 11 per group from 5–6 rats and n = 6 per group from 4 mice). $^{*}P < 0.05$, $^{**}P < 0.02$ *vs.* sham rats or L1-injected wild-type mice. $^{\#}P < 0.05$, $^{\#\#}P < 0.02$ *vs.* L5-injected wild-type mice.

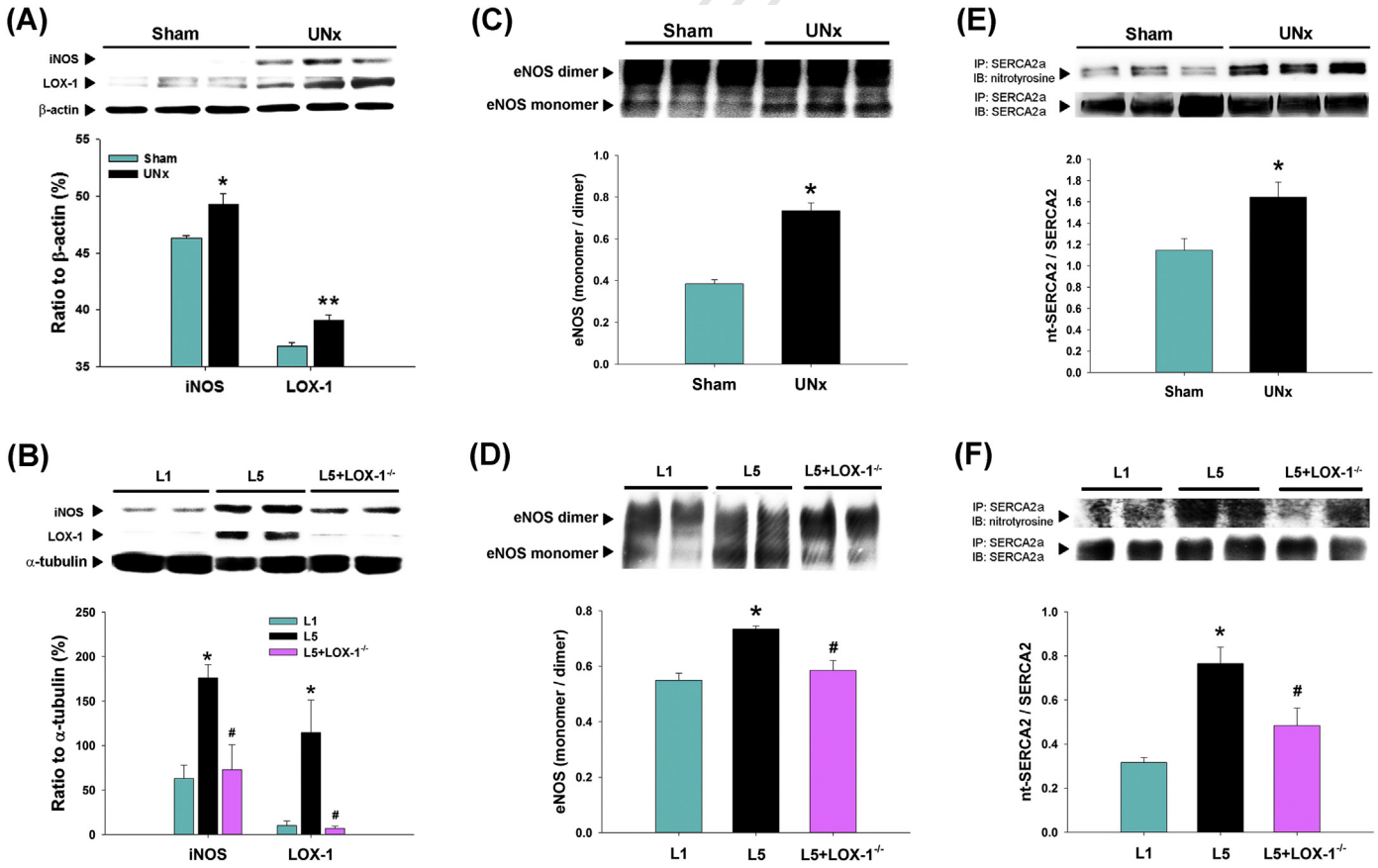

Fig. 6. Increased nitric oxide synthase-dependent SERCA2a nitrosylation in ventricular tissue from UNx rats and L5-injected mice. Representative Western blots of iNOS and LOX-1 levels and the quantitative analysis of these proteins are shown for (A) UNx and sham rats and for (B) L1- and L5-injected wild-type mice and L5-injected LOX-1$^{-/-}$ mice. Representative blots of eNOS monomer and dimer levels and the ratio of eNOS monomer levels to eNOS dimer levels are shown for (C) the 2 rat models and for (D) the 3 mouse models. The co-immunoprecipitation of nitrotyrosine with SERCA2a and the ratio of nt-SERCA2a to SERCA2a are shown for (E) the 2 rat models and for (F) the 3 mouse models. For the quantitative analyses, n = 4 per group. $^{*}P < 0.05$, $^{**}P < 0.02$ *vs.* sham rats or L1-injected wild-type mice; $^{\#}P < 0.05$ *vs.* L5-injected mice.

Please cite this article as: Chang K-C, et al, Increased LDL electronegativity in chronic kidney disease disrupts calcium homeostasis resulting in cardiac dysfunction, J Mol Cell Cardiol (2015), http://dx.doi.org/10.1016/j.yjmcc.2015.03.016

eNOS mediated the nitrosylation of SERCA2a, which may inactivate SERCA2a and impair calcium re-uptake into the sarcolemma reticulum, resulting in an intracellular calcium overload that could lead to relaxation dysfunction.

It is generally thought that during early CKD, the kidney releases humoral and/or cellular mediators that trigger maladaptive myocardial remodeling, ultimately leading to adverse cardiovascular outcomes. Several well-known mediators or triggers of this process include the renin–angiotensin system, the sympathetic nervous system, inflammation, reactive oxygen species, and nitric oxide [6]. Interestingly, our analysis suggested that the renin–angiotensin system is unaltered in early CKD. However, we discovered that alterations in LDL composition and electronegativity may be important upstream mediators of diastolic dysfunction, particularly in the early stages of CKD. Early CKD has been associated with alterations in lipoprotein metabolism, resulting in changes in apolipoproteins, lipid transfer proteins, lipolytic enzymes, and lipoprotein receptors [7]; these alterations usually precede changes in total plasma lipid levels [19]. Our data are in agreement with these findings. Although the total cholesterol, LDL cholesterol, HDL cholesterol, and triglyceride levels were similar between UNx and sham rats, we found that the LDL composition of UNx rats was different from that of sham rats. Furthermore, LDL from patients with early CKD and from UNx rats was more electronegative than LDL from controls. Moreover, the ApoB-100 in plasma LDL from patients with early CKD exhibited marked fragmentation (data not shown), which is a distinctive characteristic of L5 [20], further supporting the observation that LDL electronegativity increases in early CKD. These findings are in accordance with those of previous studies showing that patients with chronic renal failure have a different LDL phenotype than do healthy individuals [21]. Similar to findings in patients with stage 3 CKD [22], the LDL of UNx rats showed distinct differences in Apo content, including a reduction in ApoB levels; an increase in ApoAI, ApoCI, ApoCIII, and ApoE levels; and a decrease in the ratio of ApoAI to ApoCIII. In patients with CKD, the proportional increase in the levels of low-pI proteins in electronegative LDL may contribute to its overall negative charge [20,23].

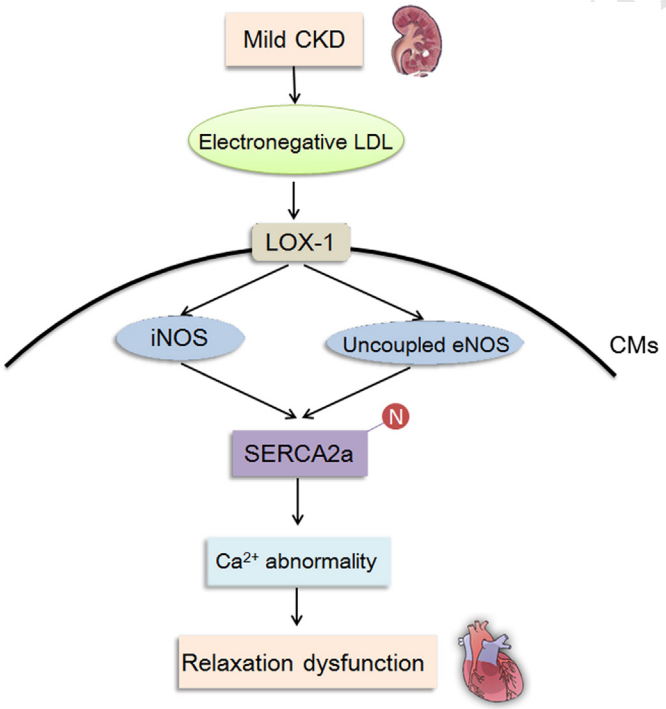

Fig. 7. Schematic summarizing the mechanisms underlying cardiac relaxation dysfunction in UNx rat model of early CKD. Arrows indicate stimulation or direction of the signaling pathway. The red circle labeled "N" denotes nitrosylation. CMs, cardiomyocytes. (For interpretation of the references to color in this figure legend, the reader is referred to the web version of this article.)

The mechanistic link between electronegative LDL and intracellular calcium overload-mediated relaxation dysfunction was supported by findings in both *in vitro* and *in vivo* experiments. LDL from UNx rats induced greater expression of LOX-1 in cardiomyocytes, which is in agreement with the effects we previously observed for L5 [8,24]. Furthermore, LDL from UNx rats stimulated iNOS production, increased nitrosylation of SERCA2a, and prolonged the calcium transient decay time *in vitro*, which supports the findings in our *in vivo* studies of UNx rat hearts. To further confirm that electronegative LDL induces calcium overload-mediated relaxation dysfunction, we injected L5 into wild-type and LOX-1$^{-/-}$ mice and examined their cardiac function *in vivo*. We found that the percentage of L5 in total LDL from patients with early CKD was 0.82 ± 0.12% (Fig. 3B), which is equivalent to an L5 plasma level of approximately 1 mg/dL. If the effects of redistribution and plasma protein binding are omitted, the dosage of L5 used to inject the mice (1 mg/kg) would presumably reach a plasma concentration of 1 mg/dL. Previously, we have found that injecting mice with 5 mg/kg of L5 causes both systolic and diastolic dysfunction of the heart and administering 2 mg/kg of L5 induces aortic senescence (our unpublished data). Therefore, in the present study, we used a lower dosage of L5 comparable to the plasma levels of L5 found in our patients with early CKD. Our results indicate that L5 induced the same relaxation dysfunction phenotype in wild-type mice that was observed in UNx rats and that this phenotype was produced *via* the same mechanism in both models; however, L5 did not induce this phenotype in LOX-1$^{-/-}$ mice. The UNx LOX-1$^{-/-}$ mice showed normal diastolic function with comparable values for the slope of EDPVR and decay tau as determined by P–V loop analysis, despite the fact that the plasma LDL of the UNx LOX-1$^{-/-}$ mice was more electronegative than that of the sham-operated LOX-1$^{-/-}$ mice. Collectively, our results suggest that highly electronegative LDL may contribute to relaxation dysfunction in early CKD *via* LOX-1-dependent signaling, which starts with an increase in iNOS and uncoupled eNOS, followed by an increase in NO-dependent nitrosylation of SERCA2a, and finally leads to intracellular calcium overload (Fig. 7).

In the current study, the diastolic dysfunction observed in UNx rat hearts was independent of myocardial fibrosis, which appears to be contradictory to the findings by Martin et al [25]. However, this discrepancy may be related to study variables such as rat species, animal size, age of the rats, left *vs.* right nephrectomy, and severity of renal insufficiency achieved. Importantly, it is also conceivable that the early diastolic dysfunction observed in mild CKD may be governed by multiple mechanisms during the course of CKD.

4.1. Limitations

Our study had a few limitations. First, our study included only one time point after UNx (i.e., 8 weeks after UNx). The UNx model represents an early and mild form of renal dysfunction and, thus, shows only mild changes in cardiac function and structure without cardiac fibrosis. The addition of another time point would lead to aging of the animals, the effects of which might outpace the effects of early CKD on cardiac remodeling. Therefore, to avoid the confounding effects of aging in our study, we assessed changes in cardiac remodeling before and 8 weeks after CKD was induced in rats. In a future study, we plan to examine whether the observed CKD-induced relaxation dysfunction seen in these rats progresses to advanced left ventricular dysfunction in a more chronic stage of CKD (i.e., >8 weeks after UNx). Second, in our *in vivo* experiments, we examined the effects of electronegative LDL on cardiac function by intravenously injecting L5 in wild-type and LOX-1$^{-/-}$ mice instead of in rats. This approach allowed us to assess the effects of L5 on cardiac remodeling in rodents and explore the role of LOX-1 signaling despite the limited amount of L5 we had available. Lastly, in the current study, we did not assess whether

Please cite this article as: Chang K-C, et al, Increased LDL electronegativity in chronic kidney disease disrupts calcium homeostasis resulting in cardiac dysfunction, J Mol Cell Cardiol (2015), http://dx.doi.org/10.1016/j.yjmcc.2015.03.016

electronegative LDL travels from the circulation to the cardiomyocytes, which would be necessary to induce cellular remodeling in the heart. Evidence suggesting this pattern of movement would support our finding that the increase in electronegative LDL associated with CKD promotes cardiac relaxation dysfunction.

4.2. Conclusions

In conclusion, we have shown that mild renal insufficiency is associated with relaxation dysfunction of the heart both in humans and in a rat model of early CKD. The operating mechanism underlying CKD-induced relaxation dysfunction involves an abnormality in calcium handling resulting from increased nitrosylation of SERCA2a, which may be driven by the alterations in LDL composition and electronegativity observed in early-stage CKD. Therapeutic interventions targeting this particular LDL phenotype may be important for reversing adverse structural and functional remodeling of the heart in early CKD.

Funding

This work was supported by grants from the American Diabetes Association [1-04-RA-13]; the NIH [HL-63364]; the Ministry of Science and Technology [NSC 100-2314-B-039-040-MY3, NSC 102-2314-B-039-019, MOST 103-2314-B-039-029, and MOST 103-2314-B-715-008]; the National Health Research Institutes of Taiwan [NHRI-EX103-10305SI and NHRI-EX104-10305SI]; the Stroke Biosignature Program Grant [BM104010092] of Academia Sinica in Taiwan; the China Medical University under the "Aim for the Top University Plan" of the Ministry of Education, Taiwan; the Taiwan Ministry of Health and Welfare Clinical Trial and Research Center of Excellence [MOHW104-TDU-B-212-113002]; Mackay Medical College [RD-1020082 and RD-1030085]; Mao-Kuei Lin Research Fund of Chicony Electronics; and Kaohsiung Medical University (KMU-TP103D09 and KMU-TP103D00).

Acknowledgments

The authors thank Nicole Stancel, PhD, ELS, and Heather Leibrecht, MS, of the Texas Heart Institute in Houston, Texas, for editorial assistance.

Disclosures

None.

Appendix A. Supplementary data

Supplementary data to this article can be found online at http://dx.doi.org/10.1016/j.yjmcc.2015.03.016.

References

[1] Ronco C, Haapio M, House AA, Anavekar N, Bellomo R. Cardiorenal syndrome. J Am Coll Cardiol 2008;52:1527–39.
[2] Manjunath G, Tighiouart H, Coresh J, Macleod B, Salem DN, Griffith JL, et al. Level of kidney function as a risk factor for cardiovascular outcomes in the elderly. Kidney Int 2003;63:1121–9.
[3] National Kidney F. K/DOQI clinical practice guidelines for chronic kidney disease: evaluation, classification, and stratification. Am J Kidney Dis 2002;39:S1–S266.
[4] Fried LF, Shlipak MG, Crump C, Bleyer AJ, Gottdiener JS, Kronmal RA, et al. Renal insufficiency as a predictor of cardiovascular outcomes and mortality in elderly individuals. J Am Coll Cardiol 2003;41:1364–72.
[5] Patel PC, Ayers CR, Murphy SA, Peshock R, Khera A, de Lemos JA, et al. Association of cystatin C with left ventricular structure and function: the Dallas Heart Study. Circ Heart Fail 2009;2:98–104.
[6] Bock JS, Gottlieb SS. Cardiorenal syndrome: new perspectives. Circulation 2010;121: 2592–600.
[7] Chan DT, Irish AB, Dogra GK, Watts GF. Dyslipidaemia and cardiorenal disease: mechanisms, therapeutic opportunities and clinical trials. Atherosclerosis 2008; 196:823–34.
[8] Chen CH, Jiang T, Yang JH, Jiang W, Lu J, Marathe GK, et al. Low-density lipoprotein in hypercholesterolemic human plasma induces vascular endothelial cell apoptosis by inhibiting fibroblast growth factor 2 transcription. Circulation 2003;107:2102–8.
[9] Chen HH, Hosken BD, Huang M, Gaubatz JW, Myers CL, Macfarlane RD, et al. Electronegative LDLs from familial hypercholesterolemic patients are physicochemically heterogeneous but uniformly proapoptotic. J Lipid Res 2007;48:177–84.
[10] Yang CY, Raya JL, Chen HH, Chen CH, Abe Y, Pownall HJ, et al. Isolation, characterization, and functional assessment of oxidatively modified subfractions of circulating low-density lipoproteins. Arterioscler Thromb Vasc Biol 2003;23:1083–90.
[11] Lee AS, Chen WY, Chan HC, Hsu JF, Shen MY, Chang CM, et al. Gender disparity in LDL-induced cardiovascular damage and the protective role of estrogens against electronegative LDL. Cardiovasc Diabetol 2014;13:64.
[12] Lu J, Jiang W, Yang JH, Chang PY, Walterscheid JP, Chen HH, et al. Electronegative LDL impairs vascular endothelial cell integrity in diabetes by disrupting fibroblast growth factor 2 (FGF2) autoregulation. Diabetes 2008;57:158–66.
[13] Chan HC, Ke LY, Chu CS, Lee AS, Shen MY, Cruz MA, et al. Highly electronegative LDL from patients with ST-elevation myocardial infarction triggers platelet activation and aggregation. Blood 2013;122:3632–41.
[14] Chang PY, Chen YJ, Chang FH, Lu J, Huang WH, Yang TC, et al. Aspirin protects human coronary artery endothelial cells against atherogenic electronegative LDL via an epigenetic mechanism: a novel cytoprotective role of aspirin in acute myocardial infarction. Cardiovasc Res 2013;99:137–45.
[15] Liang HY, Cheng WC, Chang KC. Mechanisms of right atrial pacing inducing left atrial and left ventricular dysfunction evaluated by strain echocardiography. Acta Cardiol Sin 2010;26:157–64.
[16] Zhang X, Chen C. A new insight of mechanisms, diagnosis and treatment of diabetic cardiomyopathy. Endocrine 2012;41:398–409.
[17] Lokuta AJ, Maertz NA, Meethal SV, Potter KT, Kamp TJ, Valdivia HH, et al. Increased nitration of sarcoplasmic reticulum Ca^{2+}-ATPase in human heart failure. Circulation 2005;111:988–95.
[18] Karbach S, Wenzel P, Waisman A, Munzel T, Daiber A. eNOS uncoupling in cardiovascular diseases—the role of oxidative stress and inflammation. Curr Pharm Des 2014;20: 3579–94.
[19] Attman PO, Alaupovic P. Lipid and apolipoprotein profiles of uremic dyslipoproteinemia—relation to renal function and dialysis. Nephron 1991;57:401–10.
[20] Ke LY, Engler DA, Lu J, Matsunami RK, Chan HC, Wang GJ, et al. Chemical composition-oriented receptor selectivity of L5, a naturally occurring atherogenic low-density lipoprotein. Pure Appl Chem 2011;83:1731–40.
[21] Gonen B, Goldberg AP, Harter HR, Schonfeld G. Abnormal cell-interactive properties of low-density lipoproteins isolated from patients with chronic renal failure. Metabolism 1985;34:10–4.
[22] Batista MC, Welty FK, Diffenderfer MR, Sarnak MJ, Schaefer EJ, Lamon-Fava S, et al. Apolipoprotein A-I, B-100, and B-48 metabolism in subjects with chronic kidney disease, obesity, and the metabolic syndrome. Metabolism 2004;53:1255–61.
[23] Ke LY, Stancel N, Bair H, Chen CH. The underlying chemistry of electronegative LDL's atherogenicity. Curr Atheroscler Rep 2014;16:428.
[24] Lee AS, Wang GJ, Chan HC, Chen FY, Chang CM, Yang CY, et al. Electronegative low-density lipoprotein induces cardiomyocyte apoptosis indirectly through endothelial cell-released chemokines. Apoptosis 2012;17:1009–18.
[25] Martin FL, McKie PM, Cataliotti A, Sangaralingham SJ, Korinek J, Huntley BK, et al. Experimental mild renal insufficiency mediates early cardiac apoptosis, fibrosis, and diastolic dysfunction: a kidney–heart connection. Am J Physiol Regul Integr Comp Physiol 2012;302:R292–9.

Please cite this article as: Chang K-C, et al, Increased LDL electronegativity in chronic kidney disease disrupts calcium homeostasis resulting in cardiac dysfunction, J Mol Cell Cardiol (2015), http://dx.doi.org/10.1016/j.yjmcc.2015.03.016